Biomass Conversion and Biorefinery (2023) 13:12989–12998
https://doi.org/10.1007/s13399-021-02159-5

ORIGINAL ARTICLE

Phoenix dactylifera leaf-derived biocompatible carbon quantum dots: application in cell imaging

Jegan Athinarayanan[1] · Vaiyapuri Subbarayan Periasamy[1] · Laila Naif Al-Harbi[1] · Ali A. Alshatwi[1]

Received: 15 August 2021 / Revised: 25 November 2021 / Accepted: 28 November 2021 / Published online: 20 January 2022

Abstract

Here we report a facile and eco-friendly hydrothermal method for the fabrication of carbon quantum dots (CQDs) and hydrochar from date palm leaves through integrated process. Functional groups, optical behavior, morphological features, thermal properties, and crystallinity of the synthesized CQDs were investigated using Fourier transform infrared spectroscopy, UV–vis spectroscopy, photoluminescence (PL) spectroscopy, transmission electron microscopy (TEM), thermogravimetric analyzer, and X-ray diffractometer. TEM images of CQDs revealed their spherical shape and 5–15 nm size, while PL studies demonstrated their excellent fluorescence properties. The SEM images of date palm leaf-derived hydrochar shown their sphere-shaped nature with 0.5–2 μm diameter. We investigated the cytotoxic behavior of CQDs using human mesenchymal stem cells (hMSCs) as an in vitro model with MTT assay and acridine orange/ethidium bromide (AO/EB) dual staining. The cell viability results indicate that CQDs do not significantly reduce hMSCs viability, even at a high dose (200 μg/mL). Also, AO/EB dual staining images show healthy intact nuclei in CQDs treated and untreated cells. These results confirmed the cytocompatibility and suitability of CQDs for biomedical applications. Due to CQDs fluorescent behavior, we used CQDs as fluorescent probes for cell imaging. Overall, these results demonstrate the applications of CQDs for bio-imaging of normal and cancer cells.

Keywords Carbon quantum dot · Cytocompatibility · Human mesenchymal stem cell · Cell imaging

1 Introduction

Nanostructures have attracted attention of scientific and public communities worldwide, and carbon quantum dots (CQDs) have gained remarkable importance owing to their distinct optical, electrical, catalytic, and biological behavior as well as favorable properties such as photo-bleaching resistance, low cost, solubility, extraordinary fluorescence, cell permeability, and good cytocompatibility [1–3]. As a result, CQDs have been widely used as substitutes to hazardous metal-based quantum dots and organic dyes in various applications, including cell imaging, sensing, gene transmission, catalysis, drug delivery, and optoelectronics [4]. Xu et al. first discovered CQDs during the purification of single-walled carbon nanotubes in 2004 [5]. Since then, several studies have been conducted to fabricate CQDs by approaches such as thermal decomposition, laser ablation, ultrasonication, plasma treatment, microwave, combustion, arc discharge, electrochemical exfoliation, and hydrothermal oxidation [1, 6–12]. Studies for the synthesis of CQDs have been carried out using different types of precursor materials such as lampblack, graphite, carbon soot, glycerol, resoles, ethylenediaminetetraacetic acid (EDTA), sucrose, citric acid, L-cysteine, boric acid, glycine, ethylene glycol, glucose, starch, polyethylenimine, benzene, histidine, saccharide, and polyethylene glycol [1, 8, 9, 13–18]. However, most CQD precursors are chemicals and expensive. In recent years, environmental benign, cheap, and facile methods have gained popularity for the exploitation of naturally occurring materials as sustainable precursors for CQD synthesis. A few studies have attempted CQD synthesis using renewable and sustainable materials as precursor substances, including edible chicken eggs, milk, ground coffee, water chestnut, apple juice, orange juice, sweet potatoes, garlic, shrimps, grass, orange peel, pineapple peel, oriental plane leaves,

✉ Ali A. Alshatwi
nano.alshatwi@gmail.com; alshatwi@ksu.edu.sa

[1] Nanobiotechnology and Molecular Biology Research Lab, Department of Food Science and Nutrition, College of Food and Agricultural Sciences, King Saud University, 11451 Riyadh, Kingdom of Saudi Arabia

lotus leaves, pine needles, leeks, ginkgo leaves, osmanthus leaves, palm leaves, bamboo leaves, Azadirachta indica leaves, Tridax procumbens leaves, Ocimum tenuiflorum leaves, camphor and maple leaf, cotton, oats, lychee seeds, shrimp eggs, peanut skin, coconut milk, date palm fruit, and aloe vera [19–26]. Our previous studies demonstrated that CQDs were derived from sustainable, renewable, and eco-friendly precursors including palmyra palm leaves, fish scale, and dates tree stem [1–3]. These studies have encouraged us to fabricate CQDs using naturally available cheap substances as precursors via the green chemistry approach.

Earlier studies have demonstrated the applications of CQDs as fluorescent probes for metal ion detection and cell imaging, owing to their excellent luminescence property. For instance, Li et al. reported the use of citric acid-derived CQDs for imaging of HeLa cells in blue, green, and red fluorescence emission [27]. Huang et al. employed the CQDs derived from sugarcane molasses for the imaging of breast cancer cells and to detect Fe^{3+} ions [28]. Shrimp egg-based CQDs were shown to easily enter the cytoplasm through the membrane of SK-Hep-1 cells and used for multicolor imaging [19]. *Bombyx mori* silk-derived CQDs were also found to exhibit good biocompatibility and penetrated the nucleus of A549 cells [10]. According to Zhu et al., the biocompatible and strong green fluorescence of the CQDs derived from graphene oxides may be useful in their application for biolabeling [29]. Mehta et al. suggested the use of apple juice-based CQDs as molecular probes for microbial cell imaging [30]. Wang et al. also synthesized CQDs from papaya leaf and employed them for Fe^{3+} ion sensing and *Escherichia coli* O157 and HeLa cell imaging [31]. Interestingly, Athinarayanan et al. reported that the palmyra palm leaf-derived CQDs employed as fluorescent probes for bio-imaging of human mesenchymal stem cells [2].

Phoenix dactylifera, universally well-known as date palm or date, is an ancient tree that belongs to the Arecaceae family. Mainly, the tree is commonly distributed across the Middle East, Northern Africa, and South Asia regions. In the Kingdom of Saudi Arabia, date palm tree is an important plant, and more than 25 million and 400 varieties of date palm trees are cultivated to obtain approximately 40 kg/tree of agricultural residues [32]. These agricultural residues are improperly utilized. The wastes are dumped in open sites and burnt in open places that may generate greenhouse gases, which may pollute the environment and pose health risks [33]. Hence, it is important to utilize date palm tree residues in a proper way. Although incredible progress has been made in the synthesis of CQDs, there still remains a knowledge gap in this budding field. To the best of our knowledge, no study has explored the use of date palm tree leaves for CQD and hydrochar preparation using integrated process. Herein, we attempt to fabricate CQDs and hydrochar from date palm tree leaves as renewable, sustainable, and environmentally benign precursors using integrated process. Also, we assess the CQDs cytotoxic behavior and use these CQDs as a fluorescent probe for cell imaging applications.

2 Materials and methods

2.1 Materials

The date palm tree leaves were collected from King Saud University campus, Riyadh, Kingdom of Saudi Arabia. Dulbecco's Modified Eagle's medium (DMEM), Acridine orange, ethidium bromide, trypsin–EDTA, 3-(4, 5-dimethylthiazol-2-yl)-2,5-diphenyltetrazolium bromide (MTT), and dimethyl sulfoxide (DMSO) were obtained from Sigma-Aldrich (MO, USA). Fetal bovine serum (FBS) and penicillin–streptomycin were procured from Invitrogen (Carlsbad, California. USA). The cell culture-based experiments were performed using cell culture grade chemicals.

2.2 Fabrication of CQDs

The collected date palm leaves were dried at room temperature and pulverized. The obtained powder was used as a precursor for CQD synthesis. Around 2 g of date palm leaf powder was added to 100 mL of double distilled water. The mixture was transferred to Teflon-lined hydrothermal synthesis autoclave directly kept in an oven at 180 °C for 3 h. Then, the obtained product containing solid and liquid portions was separated by centrifugation. The product was ultracentrifuged for 15 min at 20,000 rpm at 30 °C. The supernatant was carefully separated and filtered by 0.22 µm sterile filter. The liquid portion containing CQDs were dialyzed using 3.5 KD dialysis membrane (Spectrum Laboratories, USA). Then, the CQDs was freeze-dried for further analysis. The obtained solid portion was mixed with 100 mL of double distilled water and transferred to Teflon-lined hydrothermal synthesis autoclave directly kept in an oven at 200 °C for 24 h. Subsequently, the obtained brown color hydrochar was dried for further analysis.

2.3 Analysis of CQDs

The prepared CQD solution was subjected to UV–Vis spectrum analysis between 200 and 700 nm wavelength using Cary 5000 UV–Vis–NIR spectroscopy (Agilent Technologies, USA). The fluorescent behavior of the synthesized CQDs was analyzed with Jasco fluorescence spectroscopy (FP-750). Transmission electron microscopy (TEM) was used to examine the morphological features of CQDs (JEM-1011, JEOL, USA), while phase identification was carried out using an X-ray diffractometer (Rigaku MiniFlex). The surface functional groups of CQDs were analyzed with

Fourier transform infrared spectroscopy (FTIR), while their thermal behavior was evaluated with a thermogravimetric analyzer (TGA Q500, TA instruments) following a rise in temperature at a rate of 10 °C/min up to 800 °C. The synthesized CQDs were characterized using atomic force microscopy (Digital Instruments Metrology Group, model MMAFMLN) and the obtained images were analyzed with the WsXm 4.0 software (Nanotec Electronica S. L.) and Gwyddion 2.39. Scanning electron microscopy (SEM) was used to examine the morphological properties of hydrochar (JSM-7600F, JEOL, USA).

2.4 Cell culture

The hMSCs were obtained from ATCC, USA. The hMSCs were cultivated in Dulbecco's modified Eagle's medium (DMEM) supplemented with 1% antibiotics (penicillin/streptomycin) and 10% fetal bovine serum. The cell culture flask was kept in a 5% CO_2 incubator at 37 °C.

2.5 Cytotoxicity assessment

The cytotoxicity of date palm leaf-derived CQDs was evaluated using the 3-(4,5-dimethylthiazol-2-yl)-2,5-diphenyltetrazolium bromide (MTT) assay. The influence of CQDs on cell viability was studied using hMSCs as an in vitro model. hMSCs were seeded in a 96-well plate at a density of 1×10^4 cells/well and incubated overnight. The hMSCs were treated with 12.5, 25, 50, 100, and 200 µg/mL of the synthesized CQDs for 24 and 48 h, followed by the addition of 20 µL of MTT dye (5 mg/mL) per well. The plate was covered with an aluminum foil and kept in CO_2 incubator for 6 h. The media were carefully removed and the formazan products were dissolved in 200 µL of dimethyl sulfoxide (99.7%). The intensity of the colored product was monitored using a microplate reader at 570 nm (measurement) and 630 nm (reference). The received data were used to calculate percentage cell viability.

$$\text{Cell viability}(\%) = \frac{\text{Mean OD of treated cells}}{\text{Mean OD of untreated cells(control)}} \times 100$$

2.6 Influence of CQDs on cellular and nuclear morphology

About 30,000 cells/well plated in 24-well plates were incubated overnight. The cells were treated with 25, and 100 µg/mL of CQDs for 24 and 48 h. Following incubation, the media were carefully discarded and the cells were washed using phosphate-buffered saline (PBS). Subsequently, the cells were examined under a bright-field microscope.

For nuclear morphology analysis, the treated cells were stained with acridine orange (AO)/ethidium bromide (EB) dual stain (100 µg/mL of AO and EB, 1:1 ratio). The stained cells were examined under a fluorescence microscope (Carl Zeiss, Jena, Germany).

2.7 Imaging of live cells using CQDs

The cells were cultured on glass coverslips in 6-well plates. After reaching 80% confluency, the cells were treated with 25 µg/mL of CQDs for 10 h. The cells were washed twice with PBS and examined under spinning-disk confocal laser scanning microscope system (Carl Zeiss AG, Germany) at different excitation wavelengths (405, 480, and 568 nm).

3 Results and discussion

3.1 Synthesis of CQDs

Date palm tree is a vital plant in Saudi Arabia that generates a large quantity of biomass every year. This plant biomass mostly contains organic substances, including lignin, cellulose, and hemicellulose. Date palm leaves contain 47% cellulose, 16% hemicellulose, and 36% lignin [34], which attracted our attention. The leaves may serve as precursors for carbon nanostructures. Thus, in the present study, we exploited date palm leaves for CQD synthesis via hydrothermal method. During the hydrothermal treatment process, the date palm leaves were carbonized to form CQDs. Figure 1 describes the mechanism and process of CQD and hydrochar fabrication. The date palm leaves contain proteins and carbohydrates were transformed into CQDs under the pressurized condition at 180 °C.

Initially, the carbohydrates and proteins were released from date palm leaves biomass. After that, these substances were carbonized to CQDs. To purification of CQDs, the obtained liquid portion from the hydrothermal reaction was centrifuged and dialyzed. Similarly, earlier study demonstrated that palmyra palm biomass was employed as a renewable and eco-friendly precursor for preparing of CQDs [2]. The remaining solid residues were transformed into hydrochar using hydrothermal treatment at 200 °C for 24 h.

The date palm leaf-derived CQDs UV spectra are shown in Fig. 2. CQD spectra exhibited a band at 279 nm owing to $\pi \rightarrow \pi^*$ transition of electrons assigned to carbon nanostructures [35, 36]. Figure 2a inset shows the digital photograph of CQDs. After exposure to day light, CQDs turned brown in color but displayed a blue color under UV light (365 nm). Our study results strongly matched with previous studies where various renewable and eco-friendly precursors were employed for CQDs fabrication [1–3]. Generally, CQDs are synthesized using different methods, including ultrasonication, electrochemical, and microwave. These CQDs were exhibited a UV–Vis absorption band between 260 and

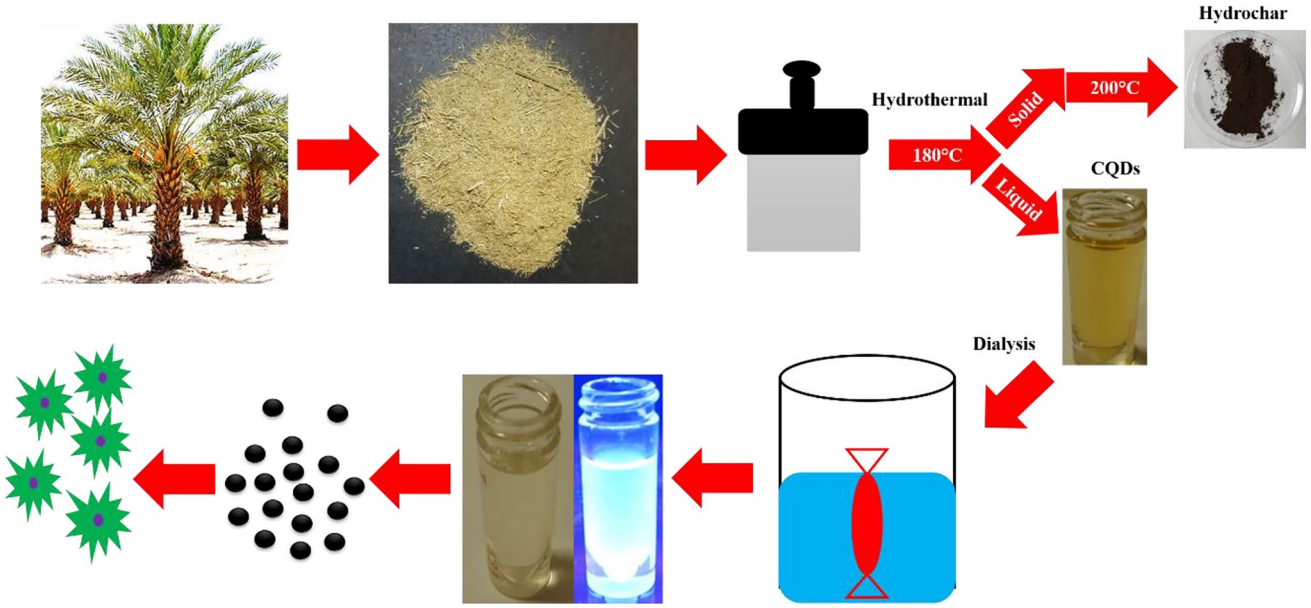

Fig. 1 Schematic presentation of CQD and hydrochar fabrication using date palm tree leaf as a sustainable carbon source for bio-imaging

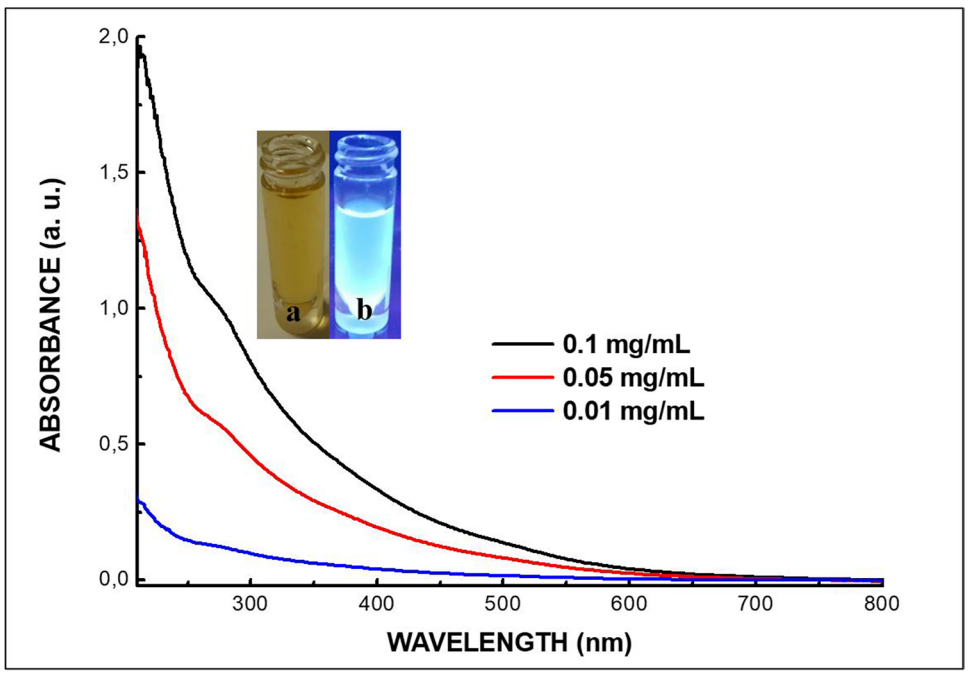

Fig. 2 UV–Vis absorption spectra of date palm tree leaf-derived CQDs (inset figure: CQDs under day light (**a**) and UV light (**b**))

320 nm, where absorption bands at longer wavelengths are generally because of surface passivation [1, 2].

The fluorescence spectra of CQDs are shown in Fig. 3. After increasing the excitation wavelength from 280 to 550 nm, the emission peak slightly shifted toward higher wavelengths and was associated with a decline in fluorescence intensity. Previous studies have reported the bathochromic shift of emission for CQDs [36, 37]. The fluorescence generation mechanism of CQDs is still unknown; however, the strong fluorescence emitted by CQDs is thought to be associated with surface passivation and quantum confinement effects [36]. Our study results revealed that date palm leaves obtained CQDs showed the excitation wavelength-based emission due to the presence of surface emissive trap states and a different size of nanoparticles [38].

Figure 4a–b shows the TEM images of date palm leaf-derived CQDs. TEM images clearly revealed that CQDs were well dispersed and spherical in shape, and had a

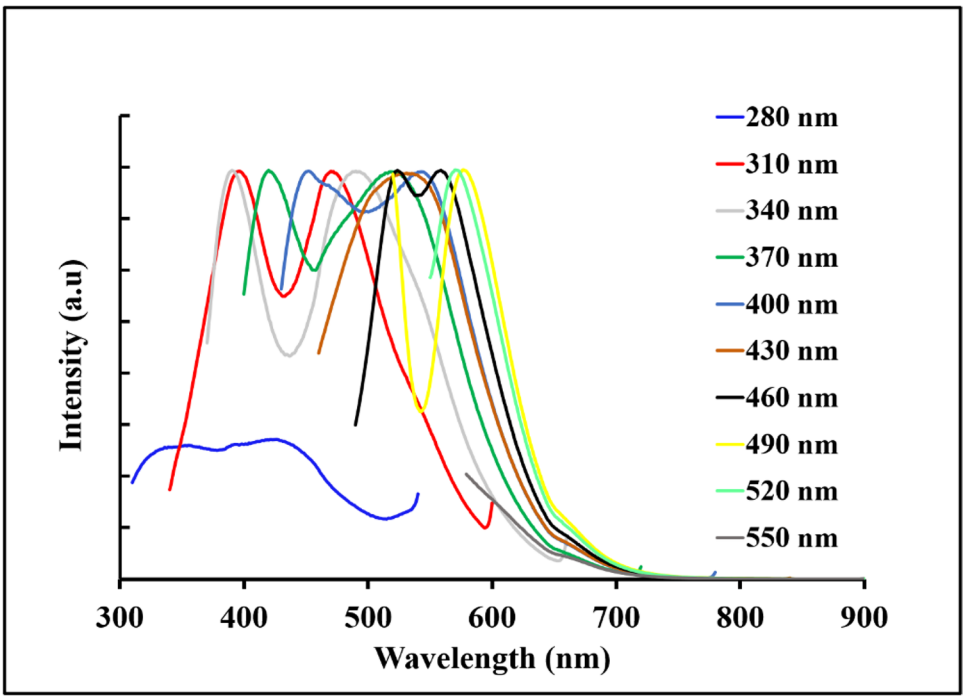

Fig. 3 Analysis of fluorescence behavior of date palm tree leaf-derived CQDs at various excitation wavelengths

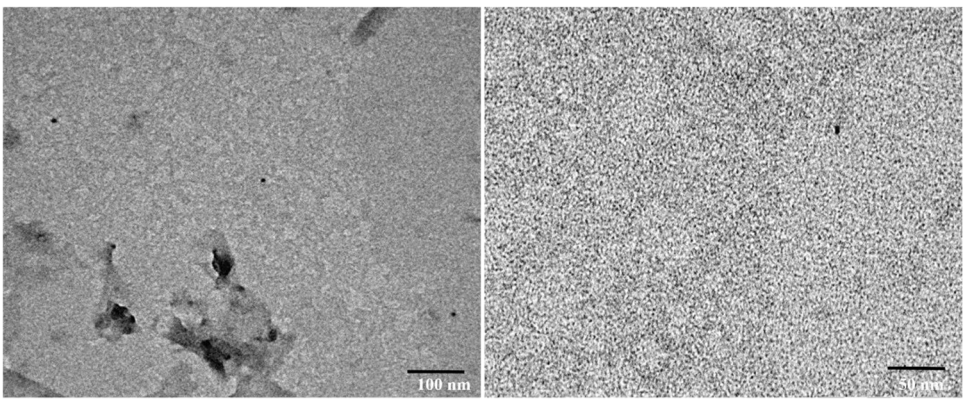

Fig. 4 **a**–**b** Transmission electron microscopy images of date palm tree leaf-derived CQDs at different magnifications

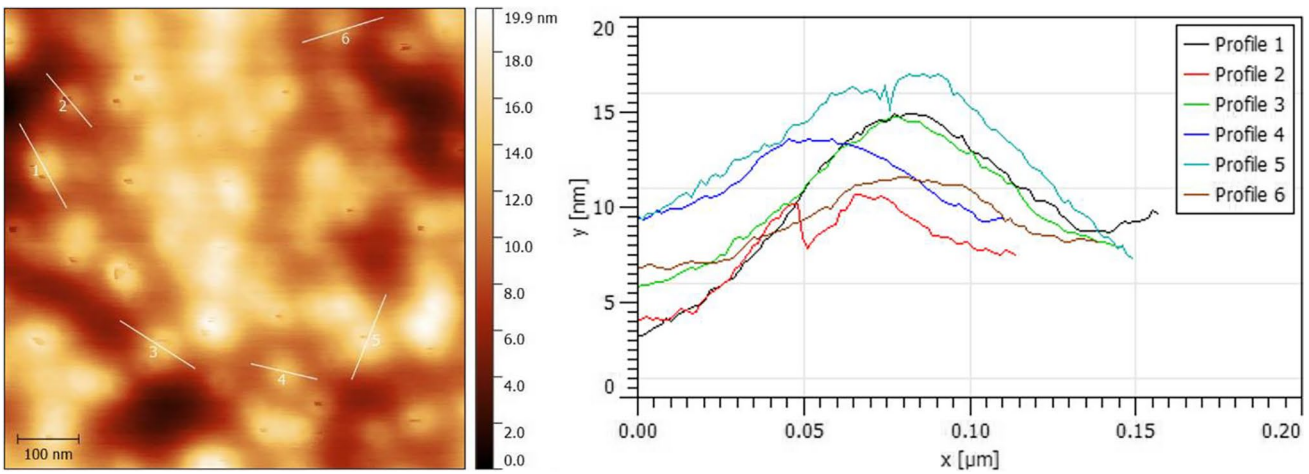

Fig. 5 Date palm leaf-derived CQDs. **a** Atomic force microscopy image and **b** height profile

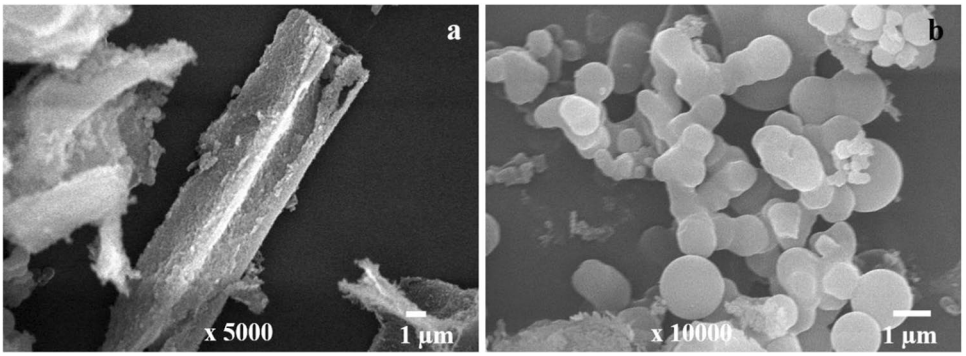

Fig. 6 **a**–**b** Scanning electron microscopy images of date palm leaf-derived hydrochar at different magnifications

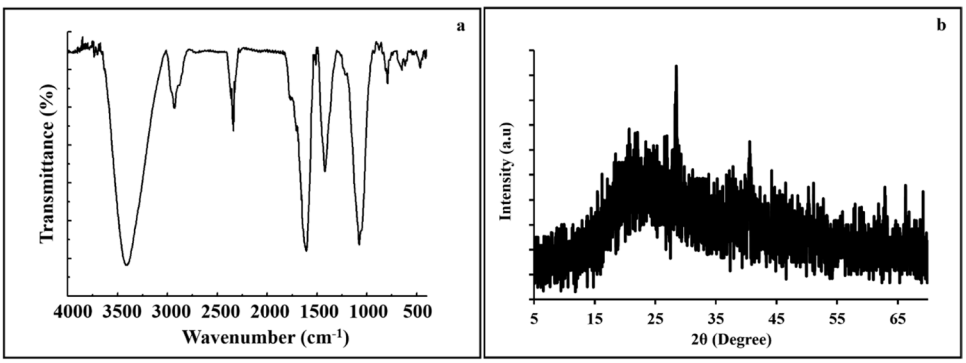

Fig. 7 **a** FTIR spectra and **b** XRD pattern of CQDs

dimeter of 5–15 nm. Atomic force microscopic images revealed the size of CQDs to be 5–15 nm (Fig. 5a–b), consistent with the results of TEM.

The morphological features of date palm leaf-derived hydrochar were analyzed using a scanning electron microscope. Figure 6a–b shows the SEM images of hydrochar. SEM images confirmed that hydrochar has a spherical shape with 0.5–2 µm diameter.

Figure 7a displays the FTIR spectrum of the synthesized CQDs, showing a broad absorption band between 3,500 and 3,400 cm^{-1}, which is related to the O–H group stretching vibration. We also observed bands around 2,950 and 1,410 cm^{-1} corresponding to C–H and C–N stretching vibrations, respectively. The band at 1,650 and 1,050 cm^{-1} was assigned to C-O stretching vibrations, indicative of the partial oxidation of CQD surface [2, 39, 40].

The X-ray diffraction (XRD) image of date palm tree leaf-derived CQDs is shown in Fig. 7b. The XRD spectrum revealed a single broad peak around 21.2°, owing to the interlayer lattice spacing of ~3.68 Å. The *d* value of CQDs was higher than that of bulk graphite (3.34 Å). Accordingly, the synthesized CQDs possessed a turbostratic carbon structure with several functional groups [41]. Earlier studies have reported similar d values for chitosan- and ethanolamine-derived CQDs [42, 43].

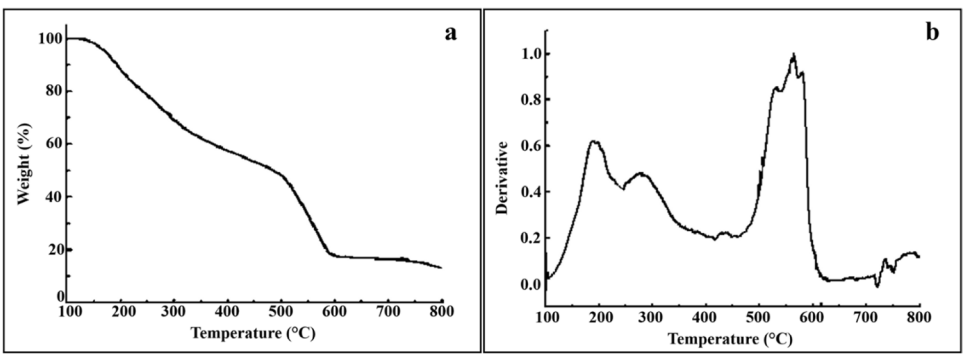

Fig. 8 **a** Thermogravimetric curve and **b** DTG curves of date palm leaf-derived CQDs

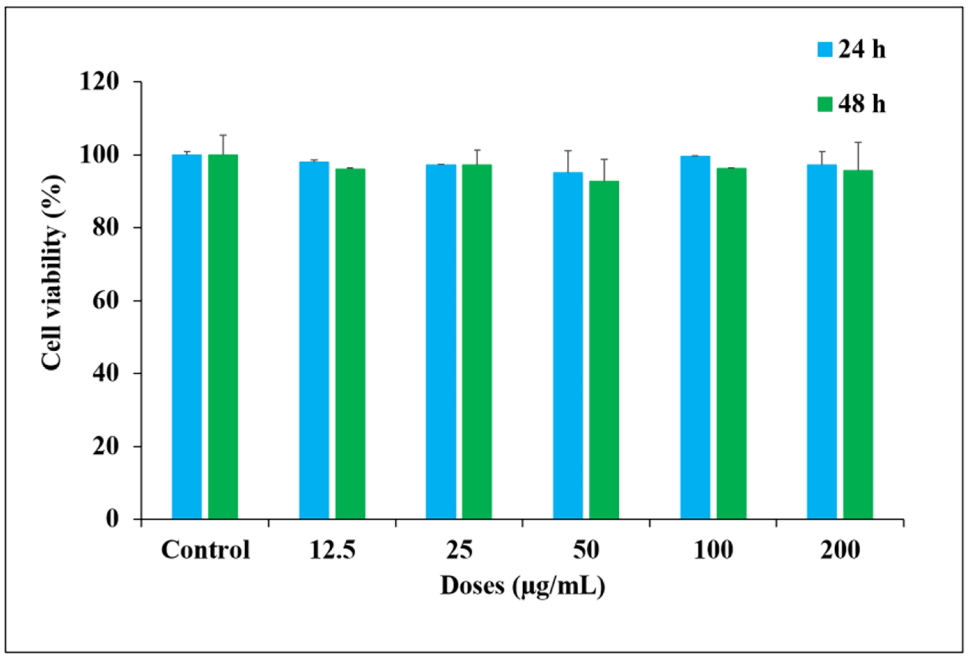

Fig. 9 Influence of CQDs on the viability of human mesenchymal stem cells after 24 and 48 h. The data represent mean ± SD of triplicates

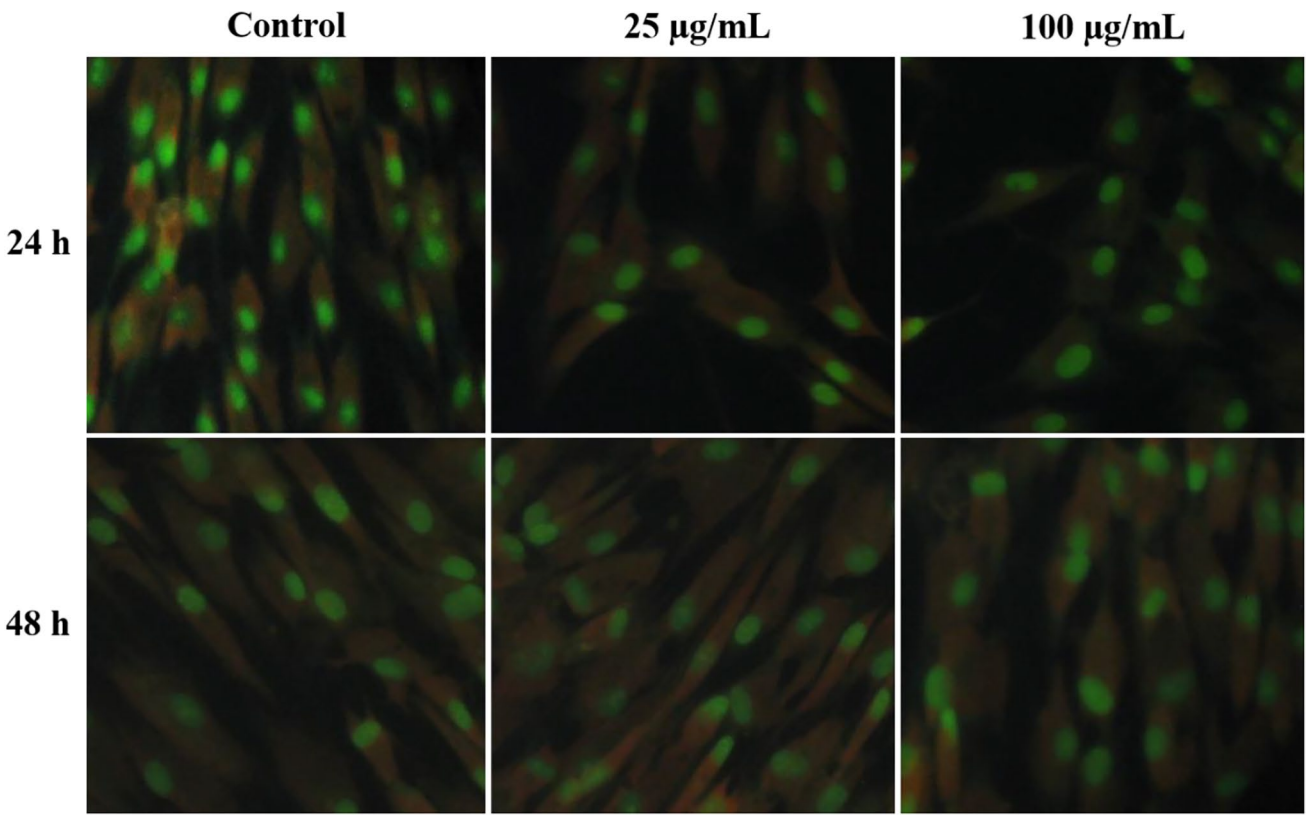

Fig. 10 Effect of CQDs on the nuclear morphology of human mesenchymal stem cells using AO/EB dual staining after 24 and 48 h

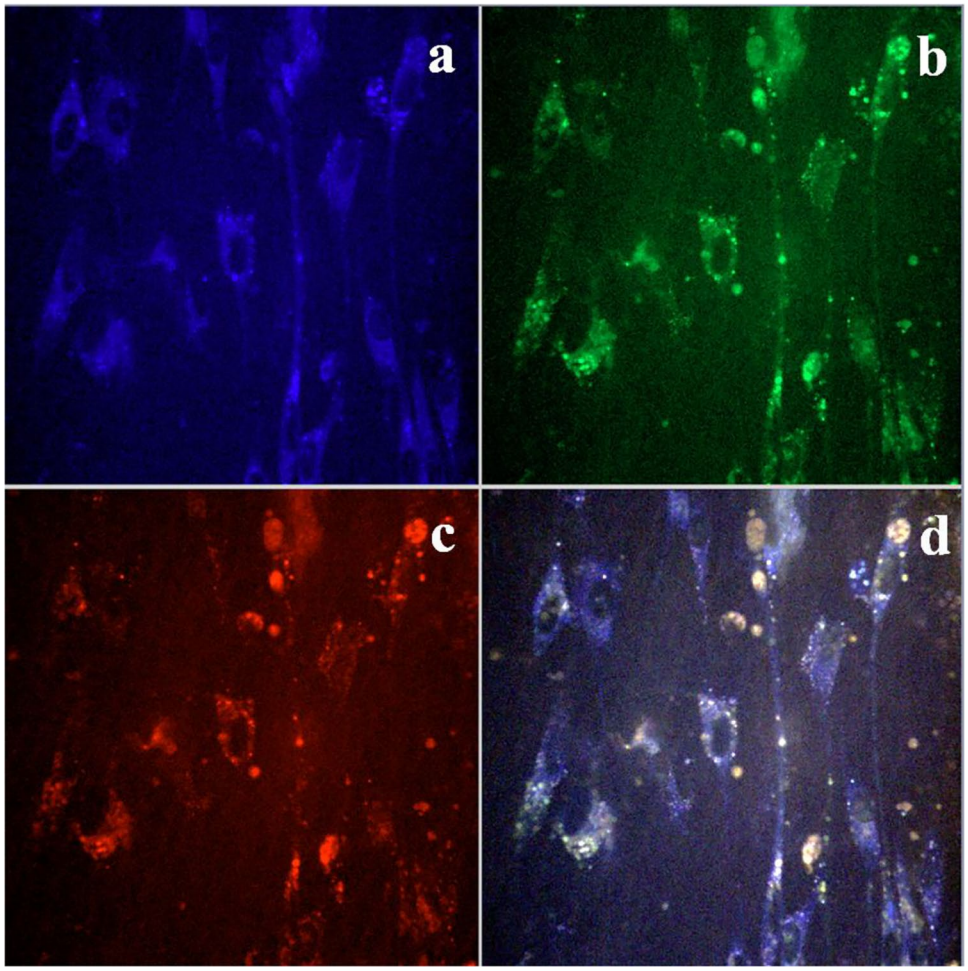

Fig. 11 Imaging of human mesenchymal stem cells using CQDs as fluorescent probes. The cells were examined under a confocal laser fluorescence microscope at different filters. **a** 405 nm, **b** 480 nm, **c** 568 nm, and **d** overlay of 405, 480, and 568 nm images

Thermogravimetric analysis (TGA and DTG) is broadly used to assess nanostructures thermal stability and surface functionalization of depending on weight loss or gained. Generally, a TGA curve is divided into different stages of decomposition: (i) the initial stage is associated with water or moisture release and (ii) the consequent stages are related to the disintegration of the structure and finally, incineration of the residual material. The thermogravimetric curve of date palm leaf-derived CQDs is shown in Fig. 8a. We observed around 9% weight loss at temperatures up to 200 °C, owing to the removal of moisture. At 300 °C, we found 30% of weight loss due to initiation of surface functional groups denaturation. Approximately 50% weight loss was noted at 500 °C because of the degradation of the organic functional groups on CQDs. We also noticed an around 30% weight loss at 500–600 °C, possibly owing to the release of pyrogas. However, no significant weight loss was observed between 600 and 800 °C. The TGA curve-associated DTG curve (Fig. 8b) displays the peak around 200 °C ascribed to the elimination of moisture, whereas the peaks at 300 °C and 550 °C were corresponding to the thermal decomposition of surface functional groups.

3.2 Cytotoxic properties of CQDs

The excitation-dependent fluorescence of the date palm-derived CQDs could be used for cell imaging applications. Previously, few studies suggested that CQDs are non-toxic and employed as different biological applications [1–3]. Cytocompatibility is an important and essential property that determines the biomedical applications of materials [44–52]. We evaluated the cytocompatibility of date palm tree leaf-derived CQDs using hMSCs as a model. The cell viability assay results are shown in Fig. 9. These results suggest that CQDs failed to remarkably alter the viability of hMSCs. Even at 200 µg/mL concentration, the viability decreased only by 1–8%, which clearly demonstrates the biocompatibility of CQDs.

Furthermore, we examined the influence of CQDs on the nuclear morphology of hMSCs using AO/EB staining (Fig. 10). We observed that the cells exposed to CQDs

showed green healthy and intact nuclei. The dual staining assay results strongly matched with the cell viability result. Earlier studies reported that non-toxic and cytocompatible nanostructured materials do not change the morphology of nucleus [1–3, 44–52]. Overall, our study results suggest that CQDs are non-toxic, biocompatible, fluorescent, and benign materials and may exhibit excellent functions in the biomedicine sector.

3.3 CQDs as fluorescent probes

We studied the labeling potential of CQDs in hMSCs with confocal laser scanning microscopy. Figure 11 shows that CQDs penetrated into the cytoplasm through the membrane of hMSCs and emitted red, green, and blue fluorescence upon excitation at 568, 480, and 405 nm. As similar, CQDs derived from different precursors were employed as a fluorescent probe [1–3]. Overall, we confirmed that CQDs exhibit good fluorescence and are non-toxic materials for biomedical applications.

4 Conclusion

The widely available, eco-friendly, and cost-effective date palm tree leaves have been used as sustainable bioprecursors for CQDs and hydrochar synthesis. The date palm leaf-derived CQDs have 5–15 nm in diameter. The hydrochar has spherical shape with 0.5–2 µm in size. The fabricated CQDs showed excellent fluorescent behavior. Also, the CQDs exhibited good biocompatibility even at 200 µg/mL. The cell imaging results revealed that CQDs outstanding performance in the label of cells. Overall, our results conclude that date palm leaf-derived CQDs can be employed for biological applications.

Funding This study was funded by the National Plan of Science, Technology and Innovation (MAARIFAH), King Abdulaziz City for Science and Technology, Kingdom of Saudi Arabia. Award Number: 15-NAN5012-02.

Declarations

Conflict of interest The authors declare no competing interests.

References

1. Athinarayanan J, Periasamy VS, Alshatwi AA (2020) Simultaneous fabrication of carbon nanodots and hydroxyapatite nanoparticles from fish scale for biomedical applications. Mater Sci Eng C 117:111313
2. Athinarayanan J, Periasamy VS, Alatiah KA, Alshatwi AA (2020) Synthesis and cytocompatibility analysis of carbon nanodots derived from palmyra palm leaf for multicolor imaging applications. Sustain Chem Pharm 18:100334
3. Athinarayanan J, Periasamy VS, Alshatwi AA (2019) Phoenix dactylifera lignocellulosic biomass as precursor for nanostructure fabrication using integrated process. Int J Biol Macromol 134:1179–1186
4. Hola K, Zhang Y, Wang Y, Giannelis EP, Zboril R, Rogach AL (2014) Carbon dots—emerging light emitters for bioimaging, cancer therapy and optoelectronics. Nano Today 9:590–603
5. Xu X, Ray R, Gu Y, Ploehn HJ, Gearheart L, Raker K, Scrivens WA (2004) Electrophoretic analysis and purification of fluorescent single-walled carbon nanotube fragments. J Am Chem Soc 126:12736–12737
6. Cao L, Wang X, Meziani MJ, Lu F, Wang H, Luo PG, Xie SY (2007) Carbon dots for multiphoton bioimaging. J Am Chem Soc 129:11318–11319
7. Sun YP, Zhou B, Lin Y, Wang W, Fernando KS, Pathak P, Jaouad MM, Harruff BA, Wang X, Wang H, Luo PG, Yang H, Erkan KM, Chen B, Veca LM, Xie SY (2006) Quantum-sized carbon dots for bright and colorful photoluminescence. J Am Chem Soc 128:7756–7757
8. Liu H, Ye T, Mao C (2007) Fluorescent carbon nanoparticles derived from candle soot. Angew Chem Int Ed Engl 46:6473–6475
9. Zhao QL, Zhang ZL, Huang BH, Peng J, Zhang M, Pang PW (2008) Facile preparation of low cytotoxicity fluorescent carbon nanocrystals by electrooxidation of graphite. Chem Commun 5116–5118
10. Wu ZL, Zhang P, Gao MX, Liu CF, Wang W, Leng F, Huang CZ (2013) One-pot hydrothermal synthesis of highly luminescent nitrogen-doped amphoteric carbon dots for bioimaging from *Bombyx mori* silk–natural proteins. J Mater Chem B 1:2868–2873
11. Zhu H, Wang X, Li Y, Wang Z, Yang F, Yang X (2009) Microwave synthesis of fluorescent carbon nanoparticles with electrochemiluminescence properties, Chem. Commun 5118–5120
12. Li H, He X, Liu Y, Huang H, Lian S, Lee ST, Kang Z (2011) One-step ultrasonic synthesis of water-soluble carbon nanoparticles with excellent photoluminescent properties. Carbon 49:605–609
13. Wang X, Long Y, Wang Q, Zhang H, Huang X, Zhu R, Teng P, Liang L, Zheng H (2013) Reduced state carbon dots as both reductant and stabilizer for the synthesis of gold nanoparticles. Carbon 64:499–506
14. Xu ZQ, Yang LY, Fan XY, Jin JC, Mei J, Peng W, Jiang FL, Xiao Q, Liu Y (2014) Low temperature synthesis of highly stable phosphate functionalized two color carbon nanodots and their application in cell imaging. Carbon 66:351–360
15. Xue W, Lin Z, Chen H, Lu C, Lin JM (2011) Enhancement of ultraweak chemiluminescence from reaction of hydrogen peroxide and bisulfite by water-soluble carbon nanodots. J Phys Chem C 115:21707–21714
16. Dong Y, Pang H, Yang HB, Guo C, Shao J, Chi Y, Li CM, Yu T (2013) Carbon-based dots co-doped with nitrogen and sulfur for high quantum yield and excitation-independent emission. Angew Chem Int Ed Engl 52:7800–7804
17. Dong Y, Wang R, Li H, Shao J, Chi Y, Lin X, Chen G (2012) Polyamine-functionalized carbon quantum dots for chemical sensing. Carbon 50:2810–2815
18. Peng H, Travas-Sejdic J (2009) Simple aqueous solution route to luminescent carbogenic dots from carbohydrates. Chem Mater 21:5563–5565
19. Lin PY, Hsieh CW, Kung ML, Chu LY, Huang HJ, Chen HT, Wu DC, Kuo CH, Hsieh SL, Hsieh S (2014) Ecofriendly synthesis

of shrimp egg-derived carbon dots for fluorescent bioimaging. J Biotechnol 189:114–119
20. Surendran P, Lakshmanan A, Vinitha G, Ramalingam G, Rameshkumar P (2020) Facile preparation of high fluorescent carbon quantum dots from orange waste peels for nonlinear optical applications. Luminescence 35:196–202
21. Sharma V, Tiwari P, Mobin SM (2017) Sustainable carbon-dots: recent advances in green carbon dots for sensing and bioimaging. J Mater Chem B 5:8904–8924
22. Rajamanikandan S, Biruntha M, Ramalingam G (2021) blue emissive carbon quantum dots (CQDs) from bio-waste peels and its antioxidant activity. J Clust Sci 1–9
23. Meena R, Singh R, Marappan G, Kushwaha G, Gupta N, Meena R, Gupta JP, Agarwal RR, Fahmi N, Kushwaha OS (2019) Fluorescent carbon dots driven from ayurvedic medicinal plants for cancer cell imaging and phototherapy. Heliyon 5:e02483
24. Zhu L, Yin Y, Wang CF, Chen S (2013) Plant leaf-derived fluorescent carbon dots for sensing, patterning and coding. J Mater Chem C 1:4925–4932
25. Tungare K, Bhori M, Racherla KS, Sawant S (2020) Synthesis, characterization and biocompatibility studies of carbon quantum dots from Phoenix dactylifera. 3 Biotech 10:1–14
26. Lim SY, Shen W, Gao Z (2015) Carbon quantum dots and their applications. Chem Soc Rev 44:362–381
27. Li L, Lu C, Li S, Liu S, Wang L, Cai W, Xu W, Yang X, Liu Y, Zhang R (2017) A high-yield and versatile method for the synthesis of carbon dots for bioimaging applications. J Mater Chem B 5:1935–1942
28. Huang G, Chen X, Wang C, Zheng H, Huang Z, Chen D, Xie H (2017) Photoluminescent carbon dots derived from sugarcane molasses: synthesis, properties, and applications. RSC Adv 7:47840–47847
29. Zhu S, Zhang J, Qiao C, Tang S, Li Y, Yuan W, Li B, Tian L, Liu F, Hu R, Gao H, Wei H, Zhang Z, Sun H, Yang B (2011) Strongly green-photoluminescent graphene quantum dots for bioimaging applications. Chem Commun 47:6858–6860
30. Mehta VN, Jha S, Basu H, Singhal RK, Kailasa SK (2015) One-step hydrothermal approach to fabricate carbon dots from apple juice for imaging of mycobacterium and fungal cells. Sens Actuators B Chem 213:434–443
31. Wang N, Wang Y, Guo T, Yang T, Chen M, Wang J (2016) Green preparation of carbon dots with papaya as carbon source for effective fluorescent sensing of Iron (III) and *Escherichia coli*. Biosens Bioelectron 85:68–75
32. Al-Abbad A, Al-Jamal M, Al-Elaiw Z, Al-Shreed F, Belaifa H (2011) A study on the economic feasibility of date palm cultivation in the Al-Hassa Oasis of Saudi Arabia. J Dev Agric Econ 3:463–468
33. Usman AR, Abduljabbar A, Vithanage M, Ok YS, Ahmad M, Ahmad M, Elfaki J, Abdulazeem SS, Al-Wabel MI (2015) Biochar production from date palm waste: charring temperature induced changes in composition and surface chemistry. J Anal Appl Pyrolysis 115:392–400
34. Nasser RA, Salem MZ, Hiziroglu S, Al-Mefarrej HA, Mohareb AS, Alam M, Aref IM (2016) Chemical analysis of different parts of date palm (*Phoenix dactylifera* L.) using ultimate, proximate and thermo-gravimetric techniques for energy production. Energies 9:374
35. Mewada A, Pandey S, Thakur M, Jadhav D, Sharon M (2014) Swarming carbon dots for folic acid mediated delivery of doxorubicin and biological imaging. J Mater Chem B 2:698–705
36. Jaiswal A, Ghosh SS, Chattopadhyay A (2012) One step synthesis of C-dots by microwave mediated caramelization of poly (ethylene glycol). Chem Commun 48:407–409
37. Zhu S, Meng Q, Wang L, Zhang J, Song Y, Jin H, Zhang K, Sun H, Wang H, Yang B (2013) Highly photoluminescent carbon dots for multicolor patterning, sensors, and bioimaging. Angew Chem Int Ed Engl 125:4045–4049
38. Ramalingam G, Kathirgamanathan P, Ravi G, Elangovan T, Manivannan N, Kasinathan K (2020) Quantum confinement effect of 2D nanomaterials. In Quantum Dots-Fundamental and Applications. Intech Open
39. Hu Y, Geng X, Zhang L, Huang Z, Ge J, Li Z (2017) Nitrogen-doped carbon dots mediated fluorescent on-off assay for rapid and highly sensitive pyrophosphate and alkaline phosphatase detection. Sci Rep 7:5849
40. Feng X, Jiang Y, Zhao J, Miao M, Cao S, Fang J, Shi L (2015) Easy synthesis of photoluminescent N-doped carbon dots from winter melon for bio-imaging. RSC Adv 5:31250–31254
41. Atchudan R, Perumal S, Edison TNJI, Pandurangan A, Lee YR (2015) Synthesis and characterization of graphenated carbon nanotubes on IONPs using acetylene by chemical vapor deposition method. Physica E Low Dimens Syst Nanostruct 74:355–362
42. Zhang J, Shu-Hong Y (2016) Carbon dots: large-scale synthesis, sensing and bioimaging. Mater Today 19:382–393
43. Han T, Yan T, Li Y, Cao W, Pang X, Huang Q, Wei Q (2015) Eco-friendly synthesis of electrochemiluminescent nitrogen-doped carbon quantum dots from diethylene triamine pentacetate and their application for protein detection. Carbon 91:144–152
44. Alshatwi AA, Athinarayanan J, Periasamy VS (2015) Biocompatibility assessment of rice husk-derived biogenic silica nanoparticles for biomedical applications. Mater Sci Eng C 47:8–16
45. Athinarayanan J, Alshatwi AA, Periasamy VS (2020) Biocompatibility analysis of Borassus flabellifer biomass-derived nanofibrillated cellulose. Carbohydr Polym 235:115961
46. Athinarayanan J, Jaafari SAAH, Periasamy VS, Almanaa TNA, Alshatwi AA (2020) Fabrication of biogenic silica nanostructures from Sorghum bicolor leaves for food industry applications. Silicon 1–8
47. Athinarayanan J, Periasamy VS, Alhazmi M, Alshatwi AA (2017) Synthesis and biocompatibility assessment of sugarcane bagasse-derived biogenic silica nanoparticles for biomedical applications. J Biomed Mater Res B Appl Biomater 105:340–349
48. Athinarayanan J, Periasamy VS, Qasem AA, Alshatwi AA (2018) Borassus flabellifer biomass lignin: isolation and characterization of its antioxidant and cytotoxic properties. Sustain Chem Pharm 10:89–96
49. Athinarayanan J, Periasamy VS, Alhazmi M, Alatiah KA, Alshatwi AA (2015) Synthesis of biogenic silica nanoparticles from rice husks for biomedical applications. Ceram Int 41:275–281
50. Athinarayanan J, Periasamy VS, Alshatwi AA (2018) Fabrication and cytotoxicity assessment of cellulose nanofibrils using Bassia eriophora biomass. Int J Biol Macromol 117:911–918
51. Athinarayanan J, Periasamy VS, Alshatwi AA (2021) Fabrication of cellulose nanocrystal-decorated hydroxyapatite nanostructures using ultrasonication for biomedical applications. Biomass Convers Biorefinery 1–14
52. Athinarayanan J, Periasamy VS, Qasem AA, Al-Shagrawi RA, Alshatwi AA (2019) Synthesis of SiO2 nanostructures from Pennisetum glaucum and their effect on osteogenic differentiation for bone tissue engineering applications. J Mater Sci Mater Med 30:1–10